JACS
JOURNAL OF THE AMERICAN CHEMICAL SOCIETY
Communication
pubs.acs.org/JACS

Linear Side Chains in Benzo[1,2-*b*:4,5-*b*′]dithiophene–Thieno[3,4-*c*]pyrrole-4,6-dione Polymers Direct Self-Assembly and Solar Cell Performance

Clément Cabanetos,[†] Abdulrahman El Labban,[†] Jonathan A. Bartelt,[‡] Jessica D. Douglas,[§] William R. Mateker,[‡] Jean M. J. Fréchet,[†,§] Michael D. McGehee,[‡] and Pierre M. Beaujuge*[,†]

[†]King Abdullah University of Science and Technology (KAUST), Thuwal 23955-6900, Saudi Arabia

[‡]Department of Materials Science and Engineering, Stanford University, Stanford, California 94305, United States

[§]Department of Chemistry and Department of Chemical and Biomolecular Engineering, University of California, Berkeley, California 94720, United States

Supporting Information

ABSTRACT: While varying the size and branching of solubilizing side chains in π-conjugated polymers impacts their self-assembling properties in thin-film devices, these structural changes remain difficult to anticipate. This report emphasizes the determining role that linear side-chain substituents play in poly(benzo[1,2-*b*:4,5-*b*′]-dithiophene–thieno[3,4-*c*]pyrrole-4,6-dione) (PBDTTPD) polymers for bulk heterojunction (BHJ) solar cell applications. We show that replacing branched side chains by linear ones in the BDT motifs induces a critical change in polymer self-assembly and backbone orientation in thin films that correlates with a dramatic drop in solar cell efficiency. In contrast, we show that for polymers with branched alkyl-substituted BDT motifs, controlling the number of aliphatic carbons in the linear *N*-alkyl-substituted TPD motifs is a major contributor to improved material performance. With this approach, PBDTTPD polymers were found to reach power conversion efficiencies of 8.5% and open-circuit voltages of 0.97 V in BHJ devices with $PC_{71}BM$, making PBDTTPD one of the best polymer donors for use in the high-band-gap cell of tandem solar cells.

Classically induced by alkyl substituents appended to the π-conjugated main chain, the solution processability of polymer donors and their intimate mixing with fullerene acceptors allow for the preparation of efficient bulk heterojunction (BHJ) solar cells.[1] Beyond the film-forming properties, nanoscale ordering in the BHJ active layer governs the material and device performance.[1c,2] Ordering aspects include (i) backbone-to-backbone self-assembly, (ii) preferential backbone orientation relative to the device substrate (i.e., "face on" vs "edge on"), (iii) paracrystalline disorder, (iv) formation of cocontinuous donor and acceptor domains and less-ordered mixed phases, and (v) ordering at the mesoscale (i.e., extended crystallinity). The degree of structural order accounts for the density of ordered domains across the BHJ, while the correlation lengths and domain sizes may vary.[2c]

Both the molecular structure of the motifs in the π-conjugated main chain[3] and the pattern of solubilizing side chains[4] are expected to direct the polymer self-assembly in thin films. Thus, changes in the size and branching of the pendant groups alter the π–π stacking and the lamellar distances between polymer backbones, which has a significant effect on the charge transport properties and in turn the device performance.[4,5] However, the factors that determine polymer crystallite orientation in thin films, implying a preferential backbone orientation relative to the device substrate, remain a matter of some debate.[3a,6] In particular, structural changes induced by the side-chain pattern are difficult to anticipate, specifically when several types of substituents are appended along the polymer backbone. Ultimately, it is expected that the ability to direct backbone orientation through material design will provide access to improved efficiencies in thin-film devices.

In this report, we examined the effect of linear side chain substitutions in poly(benzo[1,2-*b*:4,5-*b*′]dithiophene–thieno-[3,4-*c*]pyrrole-4,6-dione) (PBDTTPD) polymers (Figure 1) on both material self-assembly and solar cell performance. Earlier work showed that some of the highest open-circuit voltages (V_{OC}) (ca. 0.9 V) and fill factors (FF) (ca. 70%) can be achieved in conventional BHJ solar cells using PBDTTPD as the donor and phenyl-C61-butyric acid methyl ester (PCBM)

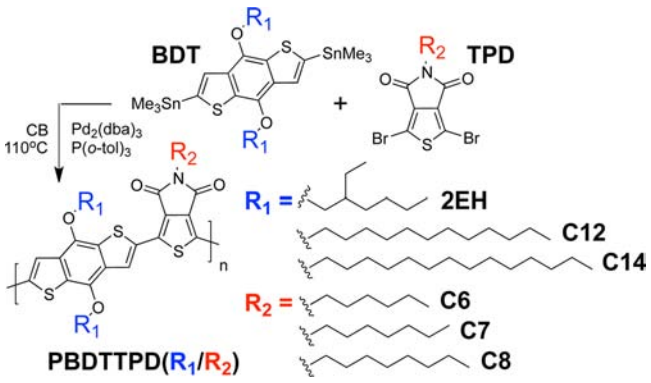

Figure 1. Synthesis of PBDTTPD(R_1/R_2) derivatives bearing alkyl side chains with various lengths and branching.

Received: January 12, 2013
Published: March 8, 2013

dx.doi.org/10.1021/ja400365b | *J. Am. Chem. Soc.* 2013, 135, 4656–4659

as the acceptor.[4a,7] In particular, the high V_{OC} and FF of PBDTTPD make it an outstanding candidate for use in the high-band-gap solar cell of tandem solar cells.[8] In this system, TPD substituents with various sizes and branching impart distinct molecular packing distances and varying degrees of nanostructural order in thin films. These structural variations have been found to correlate with solar cell efficiency, with power conversion efficiencies (PCEs) ranging from 4% to ca. 7%.[4a] Other TPD-based polymer derivatives have shown PCEs of >7%[9] and >8% in inverted devices.[10]

Since π-conjugated polymers appended with solubilizing linear *n*-alkyl solubilizing substituents can show reduced $\pi-\pi$ stacking distances between backbones and improved nanostructural order in BHJ solar cells relative to their branched-alkyl-substituted counterparts,[4a] two PBDTTPD polymers with comparable number-average molecular weights (M_n = 36/38 kDa) and polydispersity indexes (PDI ≈ 2) were synthesized: one with *n*-tetradecyl (C14)-substituted BDT and *n*-octyl (C8)-substituted TPD motifs [denoted as PBDTTPD(C14/C8)] and the other with branched 2-ethylhexyl (2EH) and C8 substituents [denoted as PBDTTPD(2EH/C8)]. Synthetic details and characterization data are given in the Supporting Information (SI). In earlier work, we showed that for linear alkyls, a greater number of aliphatic carbons is needed to impart solubilizing properties comparable to those obtained with shorter branched alkyl substituents (e.g., linear C14 substituents were shown to be appropriate alternatives to branched 2EH side chains).[11]

Thin-film BHJ solar cells with optimized PBDTTPD:$PC_{71}BM$ blend ratios (1:1.5 w/w) were fabricated from chlorobenzene (CB). The standard device architecture ITO/PEDOT:PSS/PBDTTPD:$PC_{71}BM$/Ca/Al was used throughout the study. Similar device fabrication and optimization procedures were used for all of the PBDTTPD derivatives (see the SI).

As shown in Table 1, solar cells fabricated from the control polymer PBDTTPD(2EH/C8) achieved PCEs of ca. 7%, combining a high FF of 68%, and a large V_{OC} of 0.96 V. In parallel, devices cast from blends containing 5% (v/v) of the processing additive 1-chloronaphthalene (CN) showed improved short-circuit current densities (J_{SC} = 12.5 mA/cm^2) and reached PCEs of 7.5%. Small-molecule additives such as CN and 1,8-diiodooctane (DIO) have previously been shown to help optimize the blend morphology in BHJ polymer solar cells with PCBM.[11b,12] Here, CN proved more effective than DIO in blends of PBDTTPD(2EH/C8) with $PC_{71}BM$. In contrast, solar cells made from PBDTTPD(C14/C8) using the same processing conditions showed dramatic decreases in both J_{SC} (9.1 mA/cm^2) and FF (42%); the latter could be improved to 53% using CN, albeit at the expense of J_{SC} (8.3 mA/cm^2). Overall, the PCE of the optimized devices did not exceed 4.1%, corresponding to a nearly 2-fold reduction in solar cell performance. To explore a possible correlation between the higher alkyl content in PBDTTPD(C14/C8) and material performance, a PBDTTPD derivative with *n*-dodecyl (C12)-substituted BDT motifs [PBDTTPD(C12/C8)] was synthesized following the same experimental protocol (see the SI). However, shortening the linear substituents on the BDT motifs resulted in greatly reduced solubility, thus limiting the polymer yield. Solar cells made from PBDTTPD(C12/C8) showed notably reduced J_{SC} (6.8 mA/cm^2), FF (51%), and PCE (av 3.1%), while devices cast from CN-containing blends showed even lower PCEs (av 2.5%). The current density–voltage (*J*–*V*) curves and external quantum efficiency (EQE) spectra of the optimized devices are shown in Figure 2a,b. The decreases in EQE (<50% at 550 nm) are consistent with the dramatic drops in J_{SC} observed in the solar cells made from the all-linear-alkyl-substituted polymers PBDTTPD(C14/C8) and PBDTTPD(C12/C8).

Table 1. Photovoltaic Performance of the PBDTTPD(R_1/R_2) Derivatives in Standard BHJ Devices with $PC_{71}BM$[a]

					PCE [%]	
R_1/R_2	CN[b]	J_{SC} [mA/cm^2]	V_{OC} [V]	FF	av	max
2EH/C8	N	10.8	0.96	0.68	6.9	7.0
	Y	12.5	0.93	0.65	7.3	7.5
C14/C8	N	9.1	0.90	0.42	3.3	3.4
	Y	8.3	0.93	0.53	3.8	4.1
C12/C8	N	6.8	0.92	0.51	3.1	3.2
	Y	6.5	0.89	0.45	2.5	2.6
2EH/C7	N	10.6	0.97	0.71	7.1	7.3
	Y	12.6	0.97	0.70	8.3	8.5
2EH/C6	N	8.7	0.96	0.57	4.5	4.8
	Y	11.1	0.96	0.62	6.3	6.6

[a]Optimized devices with a polymer:$PC_{71}BM$ ratio of 1:1.5 (w/w) were used. All of the devices were solution-cast from chlorobenzene (CB). [b]Devices were prepared from blends without (N) or with (Y) 5% (v/v) 1-chloronaphthalene (CN) as a processing additive.

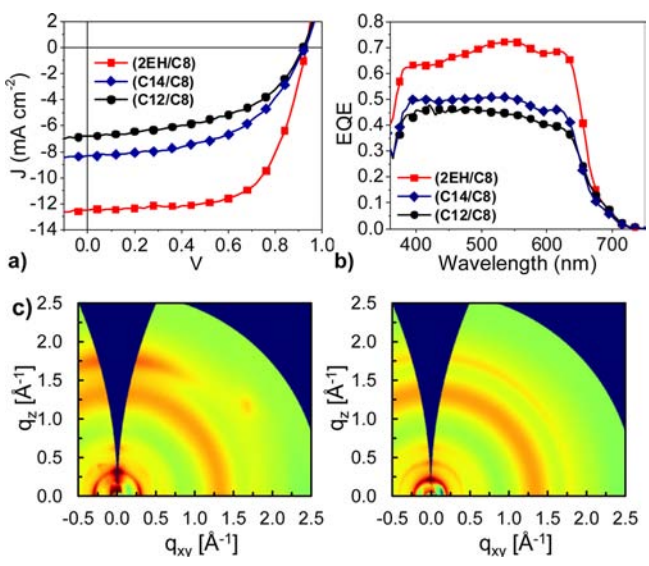

Figure 2. (a) Characteristic *J*–*V* curves of BHJ solar cells fabricated from PBDTTPD(2EH/C8), PBDTTPD(C14/C8), and PBDTTPD(C12/C8) under AM1.5G illumination (100 mW/cm^2). (b) EQE spectra of the BHJ devices. (c) GIXS patterns of (left) PBDTTPD(2EH/C8) and (right) PBDTTPD(C14/C8) in optimized BHJs with $PC_{71}BM$. The scattering intensity is plotted on a logarithmic scale and normalized in each GIXS pattern.

Grazing-incidence X-ray scattering (GIXS) data can be used to correlate polymer side-chain patterns, nanostructural order in thin films, and device performance effectively.[4] Using GIXS, we examined PBDTTPD(2EH/C8) and PBDTTPD(C14/C8) both as neat polymer films (see the SI) and in optimized BHJs with $PC_{71}BM$ (Figure 2c); all of the films were prepared from CB solutions containing 5% (v/v) CN. The GIXS data show that the two polymers adopt distinct orientations in thin films.

dx.doi.org/10.1021/ja400365b | J. Am. Chem. Soc. 2013, 135, 4656–4659

The scattering pattern of PBDTTPD(2EH/C8) shows a partial arc at $q \approx 1.76$ Å^{-1}, characteristic of $\pi-\pi$ stacking, and corresponding to a spacing of ca. 3.6 Å. The peak intensity is particularly pronounced in the out-of-plane direction ($q_{xy} \approx 0$), indicating that the polymer backbones adopt a preferential "face on" orientation relative to the substrate ($\pi-\pi$ stacking "out of plane"). Meanwhile, the partial arc shape of the peak suggests that a fraction of the polymer aggregates are somewhat misaligned with respect to the substrate. Predominantly "face-on" polymer orientations are commonly associated with higher solar cell performance.[3a,4a,11a,13] In contrast, the GIXS pattern of PBDTTPD(C14/C8) shows a nearly isotropic ring of scattering intensity at $q \approx 1.79$ Å^{-1}, which points to the absence of a preferential $\pi-\pi$ stacking orientation relative to the substrate. These intrinsic differences in backbone self-assembly and polymer orientation in thin films correlate with the drastic variations in material performance observed in BHJ solar cells with $PC_{71}BM$. In parallel, it should be noted that other morphological parameters not discussed here, such as the relative degree of crystallinity of the polymers and the purity of the domains across the active layers, may also contribute to the variations in BHJ efficiency.

In stark contrast, in PBDTTPD derivatives with branched-alkyl-substituted BDTs, such as PBDTTPD(2EH/C8), replacing branched side chains by linear ones on the TPD motifs does not significantly affect the preferential "face on" orientation of the polymers in thin films.[4a] In our effort to improve the material performance further while maintaining the same preferential polymer orientation and overall degree of structural order, we hypothesized that a fine modulation of the number of aliphatic carbons in the *N*-alkyl-substituted TPD motifs may be one of the remaining keys to improving the device PCE. It is worth noting that each methylene in the solubilizing substituent appended to TPD affects the ratio of insulating material versus active conjugated units and that reducing their number may be beneficial. On this basis, derivatives with *n*-heptyl (C7)- and *n*-hexyl (C6)-substituted TPD motifs [PBDTTPD(2EH/C7) and PBDTTPD(2EH/C6), respectively] were synthesized using the same experimental protocol (see the SI). As shown in Table 1, BHJ solar cells fabricated from PBDTTPD(2EH/C7) achieved a PCE of 7.3% (av 7.1%), combining a high J_{SC} (10.6 mA/cm^2), a slightly higher V_{OC} (0.97 V), and a high FF (71%). Importantly, devices cast from blends containing 5% (v/v) CN showed an even higher J_{SC} (12.6 mA/cm^2) while maintaining a high V_{OC} and FF, with PCEs as high as 8.5% (av 8.3%). The several batches of PBDTTPD(2EH/C7) made for the purpose of this demonstration all showed average PCEs of >7.5%, which are consistently higher than the maximum PCEs obtained with the control polymer PBDTTPD(2EH/C8). However, further shortening of the *n*-alkyl chain on TPD led to greatly reduced polymer solubility, and solution processing of PBDTTPD(2EH/C6) proved to be difficult. Optimized BHJ solar cells cast from CN-containing blends showed lower J_{SC} (11.1 mA/cm^2), FF (62%), and PCE (av 6.3%). Significantly reduced J_{SC} (8.7 mA/cm^2), FF (57%), and PCE (av 4.5%) were obtained without processing additives, pointing to inherent solution-processing limitations of the polymer. The *J*–*V* curves and EQE spectra of optimized devices are shown in Figure 3a,b. The comparably broad and efficient EQE responses for PBDTTPD(2EH/C8) and PBDTTPD(2EH/C7) (>60% over the range 370–630 nm and peaking at ca. 70% at 550 nm) are in agreement with the high J_{SC} of the solar cell devices. The EQE losses observed in the range 450–630 nm for PBDTTPD(2EH/C6) are consistent with the reduced J_{SC} and PCE (av 6.3%) of the optimized BHJ solar cells. At a first level of analysis, PBDTTPD(2EH/C8), PBDTTPD(2EH/C7), and PBDTTPD(2EH/C6) showed comparable GIXS patterns both in neat polymer films and optimized BHJs with $PC_{71}BM$ (see the SI). Quantitative X-ray analyses[2c] may provide further insight into the subtle variations of structural order across the BHJs of these polymer donors with PCBM as the acceptor.

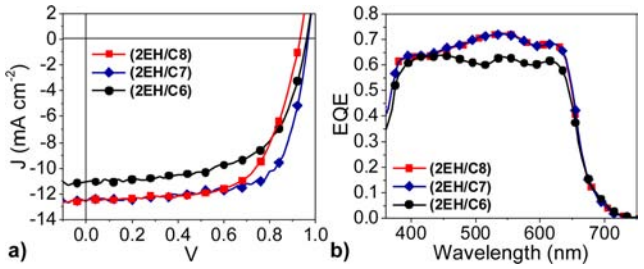

Figure 3. (a) Characteristic *J*–*V* curves of BHJ solar cells fabricated from PBDTTPD(2EH/C8), PBDTTPD(2EH/C7), and PBDTTPD-(2EH/C6) under AM1.5G illumination (100 mW/cm^2). (b) EQE spectra of the BHJ devices.

In summary, we have shown that substitutions of linear side chains in PBDTTPD polymers can greatly impact the polymer self-assembling properties and solar cell device efficiency. On the one hand, *n*-alkyl substitutions on the BDT motifs trigger a critical change of preferential polymer orientation in thin films, resulting in a dramatic drop in BHJ device PCE (<4.2%). On the other hand, in polymers with branched-alkyl-substituted BDTs, a fine modulation of the number of aliphatic carbons in the linear *N*-alkyl-substituted TPD motifs does not significantly affect the preferential backbone orientation, yet this approach shows to be a main key to improving the device performance. Thus, *N*-heptyl-substituted TPD-based polymers were found to reach PCEs of 8.5% in standard BHJ devices with $PC_{71}BM$, a significant improvement over their *N*-octyl-substituted counterparts, for which PCEs of ca. 7.5% can be achieved. This substantial increase in device performance makes PBDTTPD one of the best polymer donors for use in the high-band-gap cell of tandem solar cells.

■ ASSOCIATED CONTENT

Ⓢ Supporting Information

Synthetic details, monomer and polymer characterizations, device fabrication protocols, and additional GIXS patterns. This material is available free of charge via the Internet at http://pubs.acs.org.

■ AUTHOR INFORMATION

Corresponding Author

pierre.beaujuge@kaust.edu.sa

Notes

The authors declare no competing financial interest.

■ ACKNOWLEDGMENTS

The authors acknowledge financial support under Baseline Research Funding from KAUST. Part of this work was supported by the Center for Advanced Molecular Photovoltaics (CAMP) (Award KUS-C1-015-21) made possible by KAUST. The authors thank KAUST Analytical Core Laboratories for

mass spectrometry and elemental analyses and Dr. Michael Toney, Dr. Kristin Schmidt, and Dr. Christopher Tassone for their support with the GIXS experiments. Portions of this research were carried out at the Stanford Synchrotron Radiation Lightsource User Facility, operated by Stanford University on behalf of the U.S. Department of Energy, Office of Basic Energy Sciences.

■ REFERENCES

(1) (a) Dennler, G.; Scharber, M. C.; Brabec, C. J. *Adv. Mater.* **2009**, *21*, 1323. (b) Thompson, B. C.; Fréchet, J. M. J. *Angew. Chem., Int. Ed.* **2008**, *47*, 58. (c) Beaujuge, P. M.; Fréchet, J. M. J. *J. Am. Chem. Soc.* **2011**, *133*, 20009. (d) Zhou, H.; Yang, L.; You, W. *Macromolecules* **2012**, *45*, 607.

(2) (a) Salleo, A.; Kline, R. J.; DeLongchamp, D. M.; Chabinyc, M. L. *Adv. Mater.* **2010**, *22*, 3812. (b) Facchetti, A. *Chem. Mater.* **2011**, *23*, 733. (c) Rivnay, J.; Mannsfeld, S. C. B.; Miller, C. E.; Salleo, A.; Toney, M. F. *Chem. Rev.* **2012**, *112*, 5488.

(3) (a) Zhang, X.; Richter, L. J.; DeLongchamp, D. M.; Kline, R. J.; Hammond, M. R.; McCulloch, I.; Heeney, M.; Ashraf, R. S.; Smith, J. N.; Anthopoulos, T. D.; Schroeder, B.; Geerts, Y. H.; Fischer, D. A.; Toney, M. F. *J. Am. Chem. Soc.* **2011**, *133*, 15073. (b) Rieger, R.; Beckmann, D.; Mavrinskiy, A.; Kastler, M.; Müllen, K. *Chem. Mater.* **2010**, *22*, 5314. (c) Rieger, R.; Beckmann, D.; Pisula, W.; Steffen, W.; Kastler, M.; Müllen, K. *Adv. Mater.* **2010**, *22*, 83. (d) Guo, X.; Zhou, N.; Lou, S. J.; Hennek, J. W.; Ponce Ortiz, R.; Butler, M. R.; Boudreault, P.-L. T.; Strzalka, J.; Morin, P.-O.; Leclerc, M.; López Navarrete, J. T.; Ratner, M. A.; Chen, L. X.; Chang, R. P. H.; Facchetti, A.; Marks, T. J. *J. Am. Chem. Soc.* **2012**, *134*, 18427. (e) Scharber, M. C.; Koppe, M.; Gao, J.; Cordella, F.; Loi, M. A.; Denk, P.; Morana, M.; Egelhaaf, H.-J.; Forberich, K.; Dennler, G.; Gaudiana, R.; Waller, D.; Zhu, Z.; Shi, X.; Brabec, C. J. *Adv. Mater.* **2010**, *22*, 367.

(4) (a) Piliego, C.; Holcombe, T. W.; Douglas, J. D.; Woo, C. H.; Beaujuge, P. M.; Fréchet, J. M. J. *J. Am. Chem. Soc.* **2010**, *132*, 7595. (b) Mei, J.; Kim, D. H.; Ayzner, A. L.; Toney, M. F.; Bao, Z. *J. Am. Chem. Soc.* **2011**, *133*, 20130.

(5) (a) Beaujuge, P. M.; Pisula, W.; Tsao, H. N.; Ellinger, S.; Müllen, K.; Reynolds, J. R. *J. Am. Chem. Soc.* **2009**, *131*, 7514. (b) Beaujuge, P. M.; Tsao, H. N.; Hansen, M. R.; Amb, C. M.; Risko, C.; Subbiah, J.; Choudhury, K. R.; Mavrinskiy, A.; Pisula, W.; Brédas, J.-L.; So, F.; Müllen, K.; Reynolds, J. R. *J. Am. Chem. Soc.* **2012**, *134*, 8944. (c) Coffin, R. C.; Peet, J.; Rogers, J.; Bazan, G. C. *Nat. Chem.* **2009**, *1*, 657. (d) Ko, S.; Verploegen, E.; Hong, S.; Mondal, R.; Hoke, E. T.; Toney, M. F.; McGehee, M. D.; Bao, Z. *J. Am. Chem. Soc.* **2011**, *133*, 16722. (e) Yang, L.; Zhou, H.; You, W. *J. Phys. Chem. C* **2010**, *114*, 16793.

(6) (a) Rivnay, J.; Steyrleuthner, R.; Jimison, L. H.; Casadei, A.; Chen, Z.; Toney, M. F.; Facchetti, A.; Neher, D.; Salleo, A. *Macromolecules* **2011**, *44*, 5246. (b) Rivnay, J.; Toney, M. F.; Zheng, Y.; Kauvar, I. V.; Chen, Z.; Wagner, V.; Facchetti, A.; Salleo, A. *Adv. Mater.* **2010**, *22*, 4359. (c) Steyrleuthner, R.; Schubert, M.; Howard, I.; Klaumünzer, B.; Schilling, K.; Chen, Z.; Saalfrank, P.; Laquai, F.; Facchetti, A.; Neher, D. *J. Am. Chem. Soc.* **2012**, *134*, 18303.

(7) (a) Aïch, B. R.; Lu, J.; Beaupré, S.; Leclerc, M.; Tao, Y. *Org. Electron.* **2012**, *13*, 1736. (b) Hoke, E. T.; Vandewal, K.; Bartelt, J. A.; Mateker, W. R.; Douglas, J. D.; Noriega, R.; Graham, K. R.; Fréchet, J. M. J.; Salleo, A.; McGehee, M. D. *Adv. Energy Mater.* **2013**, *3*, 220. (c) Bartelt, J. A.; Beiley, Z. M.; Hoke, E. T.; Mateker, W. R.; Douglas, J. D.; Collins, B. A.; Tumbleston, J. R.; Graham, K. R.; Amassian, A.; Ade, H.; Fréchet, J. M. J.; Toney, M. F.; McGehee, M. D. *Adv. Energy Mater.* **2013**, *3*, 364.

(8) Beiley, Z. M.; McGehee, M. D. *Energy Environ. Sci.* **2012**, *5*, 9173.

(9) Chu, T.-Y.; Lu, J.; Beaupré, S.; Zhang, Y.; Pouliot, J.-R.; Zhou, J.; Najari, A.; Leclerc, M.; Tao, Y. *Adv. Funct. Mater.* **2012**, *22*, 2345.

(10) (a) Amb, C. M.; Chen, S.; Graham, K. R.; Subbiah, J.; Small, C. E.; So, F.; Reynolds, J. R. *J. Am. Chem. Soc.* **2011**, *133*, 10062. (b) Small, C. E.; Chen, S.; Subbiah, J.; Amb, C. M.; Tsang, S.-W.; Lai, T.-H.; Reynolds, J. R.; So, F. *Nat. Photonics* **2012**, *6*, 115.

(11) (a) Yiu, A. T.; Beaujuge, P. M.; Lee, O. P.; Woo, C. H.; Toney, M. F.; Fréchet, J. M. J. *J. Am. Chem. Soc.* **2012**, *134*, 2180. (b) Woo, C. H.; Beaujuge, P. M.; Holcombe, T. W.; Lee, O. P.; Fréchet, J. M. J. *J. Am. Chem. Soc.* **2010**, *132*, 15547.

(12) (a) Peet, J.; Kim, J. Y.; Coates, N. E.; Ma, W. L.; Moses, D.; Heeger, A. J.; Bazan, G. C. *Nat. Mater.* **2007**, *6*, 497. (b) Lee, J. K.; Ma, W. L.; Brabec, C. J.; Yuen, J.; Moon, J. S.; Kim, J. Y.; Lee, K.; Bazan, G. C.; Heeger, A. J. *J. Am. Chem. Soc.* **2008**, *130*, 3619. (c) Hoven, C. V.; Dang, X.-D.; Coffin, R. C.; Peet, J.; Nguyen, T.-Q.; Bazan, G. C. *Adv. Mater.* **2010**, *22*, E63.

(13) Guo, J.; Liang, Y.; Szarko, J.; Lee, B.; Son, H. J.; Rolczynski, B. S.; Yu, L.; Chen, L. X. *J. Phys. Chem. B* **2010**, *114*, 742.